An Experimental Study on the Dynamic Hysteresis Behavior of a Magnetic Soft Continuum Robot Submerged in a Fluid Environment

Conference Paper · May 2024

CITATIONS
0

READS
120

3 authors, including:

Alireza Moezi
Concordia University
37 PUBLICATIONS **544** CITATIONS

SEE PROFILE

Proceedings of the Canadian Society for Mechanical Engineering International Congress
31st Annual Conference of the Computational Fluid Dynamics Society of Canada
CSME/CFD2024
May 26–29, 2024, Toronto, Ontario, Canada

An Experimental Study on the Dynamic Hysteresis Behavior of a Magnetic Soft Continuum Robot Submerged in a Fluid Environment

Seyed Alireza Moezi[1*], Ramin Sedaghati[1], Subhash Rakheja[1]
[1]Department of Mechanical, Industrial & Aerospace Engineering, Concordia University, Montreal, Canada
*seyedalireza.moezi@concordia.ca

Abstract— In recent years, Magnetic Soft Continuum Robots (MSCRs) have gained significant attention partly due to their promising applications in sensitive and precise biomedical tasks, such as targeted drug delivery and minimally invasive treatments. These applications benefit from the unique multimodal locomotion of MSCRs and their wireless actuation capabilities. MSCRs typically undergo large deformation when subjected to magnetic fields. However, there are very limited studies on characterizing their nonlinear hysteresis behavior, especially in fluid environments subjected to varying magnetic field. This study attempts to experimentally investigate the real-time nonlinear and hysteretic behaviors of an MSCR (designed as a cantilever beam made of magnetoactive elastomer) fully submerged in a fluid environment. The MSCR's behavior is explored under both DC and AC magnetic intensities. In AC scenarios, the robot experiences a high oscillatory magnetic field, ranging from 5 to 25 mT, and is subjected to frequencies as high as 5 Hz. To generate a uniform and precise magnetic field, a hardware-in-the-loop experiment employing a feedforward-PID controller was designed. The experimental data were subsequently analyzed to realize the MSCR's response time histories and hysteretic responses.

Keywords- magnetic soft robot; feedforward-PID control algorithm; hardware-in-the-loop experiment; large deformation; high-frequency oscillatory movements.

I. INTRODUCTION

Magnetic Soft Continuum Robots (MSCRs) have shown significant potential in a variety of applications [1–5]. Their wireless actuation, ability to achieve sub-millimeter scale, and multimodal locomotion capabilities under low magnetic fields make them well-suited for biomedical applications such as targeted drug delivery, minimally invasive surgery, and cell transportation. MSCRs are typically fabricated using methods like molding, lost-wax casting, and 4D printing, which involve embedding hard ferromagnetic particles, such as neodymium-iron-boron, in a soft elastomeric matrix [6]. Owing to their elastomeric nature, MSCRs can achieve large deformations, a feature advantageous in complex and confined environments like human arteries.

Dynamic characterization and thorough investigation are essential for comprehending the complex and highly nonlinear behavior of soft magnetic actuators. Some efforts have been made to simulate soft magnetic actuators to understand their nonlinear behavior under various magnetic stimuli [6–15]. Zhao et al. [7] utilized ABAQUS software to assess the large deformation of a magnetic soft actuator. Moezi et al. [8] developed an FE model within COMSOL Multiphysics software to examine the dynamic behavior of a magnetic soft robot. Chen et al. [9] formulated a mathematical model for predicting the static deformation of a hard-magnetic soft actuator. Dadgar-Rad and Hossain [10] investigated the time-dependent deformation of magnetic soft actuators, which comprise hard ferromagnetic particles. Kadapa et al. [11] established a theoretical constitutive model for an iron-enriched magneto-active polymer to study its nonlinear behaviors. Xing and Yong [12] designed an analytical model to calculate the longitudinal deformation of a hard-magnetic soft actuator under DC and AC magnetic forces. Nagal et al. [13] modeled the Gent hyperelastic model to study the deformation of a magnetoactive soft actuator. Moezi et al. [14] later developed an exact nonlinear dynamic model, accompanied by experimental studies, to examine the large deformations of a hard-magnetic soft actuator subjected to various AC and DC magnetic fields. Additionally, they investigated the hysteretic response of the fabricated beam when exposed to low-frequency magnetic fields. In another study, Moezi et al. [15] developed a nonlinear dynamic model and model-based AI-driven control strategy to investigate the behavior and control of a magnetoactive soft continuum robot in a fluidic environment. They also [6] investigated the hysteretic response of a hard-magnetic soft actuator under the presence of an oscillatory magnetic field with frequencies of up to 3 Hz.

Despite these advancements, most studies have focused on quasi-static analysis. The dynamic response of magnetic soft actuators, especially under high-frequency magnetic fields, has rarely been reported [6], especially in fluidic environments. Motivated by the aforementioned limitations and the significant potential of magnetic soft actuators, this study presents an experimental investigation into the nonlinear dynamic hysteresis behavior of a fabricated MSCR. The study specifically aims to

investigate the nonlinear response behavior of the MSCR when submerged in a fluidic environment and subjected to high-frequency, uniform magnetic fields. The MSCR was fabricated through a molding technique, and its mechanical properties were determined using a tensile test. A hardware-in-the-loop (HiL) experiment was conducted to explore the MSCR's dynamic responses to magnetic stimuli at higher frequencies and assess the effect of rate-dependent hysteresis. A Feedforward-PID controller, established within the Simulink Real-Time environment, was utilized to regulate the magnetic flux density, ensuring its precision and uniformity. The collected data were analyzed to understand the MSCR's time-dependent and hysteretic responses. The structure of the manuscript is as follows: Section 2 outlines the proposed system in this study, Section 3 details the fabrication process and the design of the experiment, Section 4 presents and discusses the experimental findings and the final section summarizes the conclusions of the present study.

II. PROBLEM STATEMENT

The magnetic soft continuum robot in this study is modeled as a cantilevered actuator fully submerged in a fluid and exposed to a uniform magnetic field, **H**. This field is applied perpendicularly to the length of the beam, as depicted in Figure 1. In its static equilibrium state, the MSCR's residual magnetic flux density, **M**, is presumed to align along the x-axis. Additionally, Figure 1 highlights **B**, representing the induced magnetic flux density caused by the external magnetic field **H** within the magnetoactive soft robot.

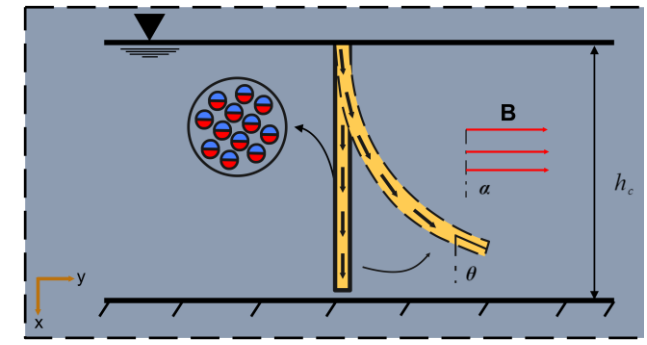

Figure 1. Schematic of the magnetic soft continuum robot submerged in a fluid environment under a uniform magnetic field.

III. MATERIALS AND METHODS

A. Sample Preparation and Characterizations

The MSCR was fabricated by embedding hard magnetic NdFeB particles (MQFP-B+, Neo-Magnequench) with a diameter of 5 micrometers into a soft matrix of Ecoflex 0050 (Smooth-On, Inc). Initially, Ecoflex 0050 – Part A was mixed with Part B from the same manufacturer in a 1:1 mass ratio, maintaining the iron particles at a volume fraction of 20%. These NdFeB particles were evenly blended into the uncured liquid silicone-based resin using a vacuum mixer (Thinky: ARV-200) under a controlled vacuum pressure of 26 inHg and an angular velocity of 2000 rpm for 40 seconds. A precise rectangular mold, accurate to 25 microns, was fabricated using an SLA 3D printer (Formlabs Form 3+) and impregnated with a release agent (Ease Release 200, Smooth-On-Inc). The mixture was then poured into this mold and cured in an oven at 200°F for approximately 30 minutes. The final MSCR dimensions (as listed in Table I) were achieved by removing the cured sample from the mold with a razor cutter. The sample was then magnetized along its length using a strong magnetic field (1.7 T) generated by a variable airgap electromagnet (DXSBV-100, Dexing Magnet Tech. Co., Limited) with 4 cm poles. Figure 2 summarizes the fabrication process.

The mechanical properties of the magnetized sample were determined through laboratory tests. The sample underwent tensile testing at a displacement rate of 500 mm/min until failure using a uniaxial loading test system (F1505-IM, Mark–10). The resulting data provided the stress-stretch characteristics of the sample, as shown in Figure 3. This data was then fitted to the Mooney-Rivlin hyperelastic model [16] to derive the mechanical properties of the MSCR. Table 1 shows the mechanical properties of the MSCR sample.

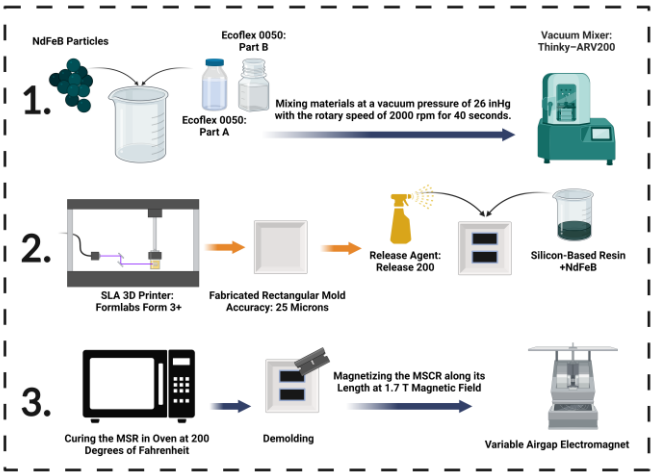

Figure 2. Processes used for (1) fabrication of MSCR sample, (2) fabrication of mold and molding process, and (3) curing and magnetizing of the sample.

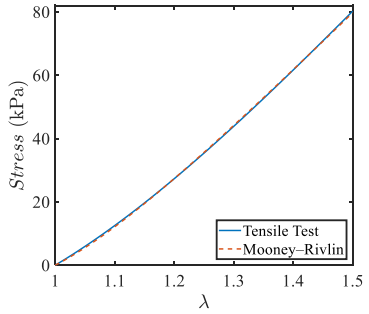

Figure 3. The stress-stretch response of the MSCR sample obtained from the tensile test and the fitted Mooney-Rivlin model.

TABLE I. GEOMETRICAL AND MECHANICAL PROPERTIES OF THE MSCR SAMPLE.

Parameter	Value	Parameter	Value
Length (mm)	8	Poisson's ratio	0.499
Width (mm)	3.7	Young's modulus (kPa)	97.813
Thickness (mm)	1.07	Shear modulus (kPa)	32.626

B. *Measurements of Magneto-Viscoelastic Responses*

Two sets of experiments were conducted to assess the magneto-viscoelastic behaviors of the fabricated MSCR when exposed to a range of quasi-static and dynamic magnetic fields. The initial set focused on determining the responses of the MSCR to quasi-static magnetic fields. The second set investigated the MSCR's dynamic responses to various uniform oscillatory magnetic fields. The data collected from these experiments were subsequently analyzed to understand the MSCR's dynamic response to harmonic magnetic stimuli at frequencies varying from 0.25 to 5 Hz. The experiments utilized harmonic magnetic stimuli ranging from 5 to 25 mT, produced by a 3D Helmholtz coil system (Woodruff Scientific), which was powered by three servo amplifiers (AB100C200, Advanced Motion Controls). The magnetic field around the MSCR was measured using a portable gauss meter (Parker 5180, F.W. BELL) and collected using a data acquisition card (M Series–NI PCI-6259, National Instruments). To capture the magneto-viscoelastic behavior of the MSCR at its free end, a high-speed CXP camera (boA2832-190cc, Basler) was employed, with the data being recorded through a dedicated real-time frame grabber (CXP-12 Quad, Basler) and analyzed with an image processing algorithm developed in Python using the OpenCV framework. A HiL experiment was designed to observe the MSCR's real-time nonlinear response, as shown in Figure 4. A Feedforward-PID control algorithm, outlined in Figure 5 and implemented in MATLAB-Simulink Real-Time (R2017a) with a sample time of 0.002 seconds, allowed for providing a uniform and precise magnetic field during the experiments. For experimental tests, a phantom was designed using SOLIDWORKS 2022 and then fabricated with an SLA 3D printer (Formlabs Form 3+) utilizing clear resin (V4). This printed phantom was then finely sanded and coated with a clear finish (Max 2K–Clear Glamour, SprayMax). The design of the 3D-printed phantom featured an 80 mm-long channel with a cross-section measuring 10×10 mm². In these experiments, a fluid mixture comprising water and glycerol (G33-4, Fisher Chemical) was utilized.

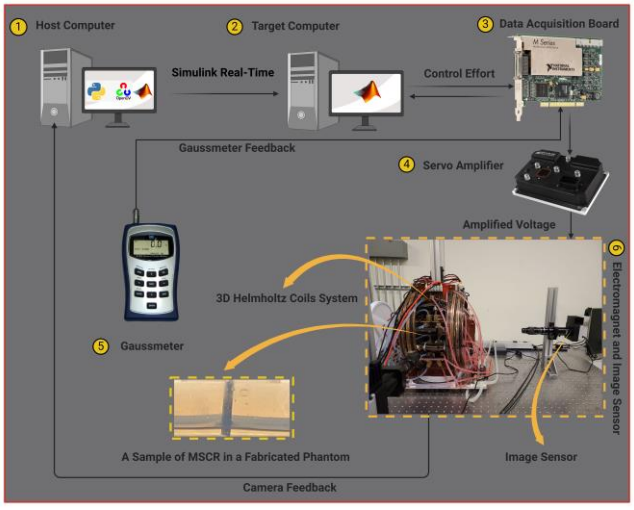

Figure 4. HiL experiment design for real-time actuation of the MSCR.

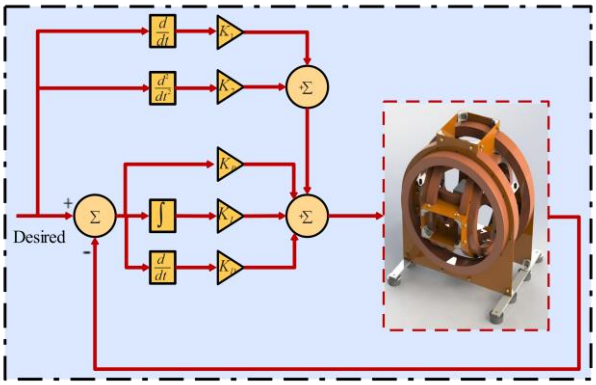

Figure 5. Schematic of the Feedforward-PID control algorithm.

IV. Results and Discussion

A. *Quasi-static Response Characteristics of MSCR*

The quasi-static response behavior of the MSCR was assessed to capture its large deflection at the free end when subjected to uniform magnetic stimuli perpendicular to the MSCR's x-axis. Figure 6 displays the angular deformation of the MSCR under the quasi-static magnetic intensity ranging from 2 mT to 25 mT. Results in Figure 6 are also quantified in Table 2. As indicated in both Figure 6 and Table 2, the MSCR demonstrates a distinctly nonlinear response, with a noticeable trend towards saturation.

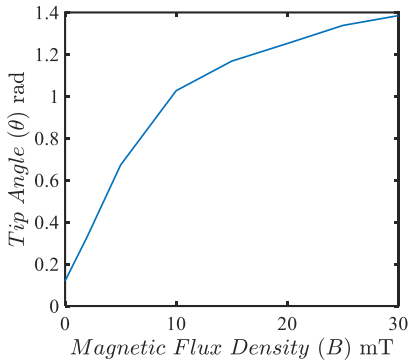

Figure 6. Angular deflections of the MSCR's free-end measured for different magnetic flux intensities.

TABLE II. Angular deformation of the MSCR's free-end under different magnitudes of magnetic intensities.

Magnetic Flux Density (mT)	Tip Deflection in radian
2	0.33
5	0.67
10	1.03
15	1.17
20	1.25
25	1.34
30	1.39

B. *Dynamic Response of the MSCR Under Oscillatory Magnetic Loads*

The dynamic behavior of the MSCR was evaluated by applying various harmonic magnetic loads. The experiments were conducted with ten different magnetic field excitations,

where the amplitude of the magnetic flux density varied from 5 to 25 mT across a frequency range of 0.25 Hz to 5 Hz. These specific excitation scenarios, labeled as C.1, C.2, ..., C.10, are tabulated in Table 3. The response of the MSCR's tip deflection was recorded for each case over a period of 30 seconds. It is noted that to enhance the clarity of the recorded responses, a zero-phase digital filter was employed in MATLAB (R2023a) to refine the measured data.

TABLE III. HARMONIC MAGNETIC FIELD PROFILES CONSIDERED FOR CHARACTERIZING THE DYNAMIC RESPONSE OF FABRICATED MSCR.

Case	Magnetic field excitation	Case	Magnetic field excitation
C.1	5 sin(2πt)	C.6	15 sin(4πt)
C.2	5 sin(4πt)	C.7	15 sin(6πt)
C.3	5 sin(6πt)	C.8	15 sin(10πt)
C.4	5 sin(10πt)	C.9	25 sin($t\pi$/2)
C.5	15 sin(2πt)	C.10	25 sin(3πt)

Figure 7 presents the time histories of the MSCR's free-end angular deformation for various magnetic excitation scenarios outlined in Table 3. The time history responses exhibit minor asymmetries, potentially due to a slight initial curvature of the MSCR, imperfections in the experimental setup and fixture, minor non-uniformities in the magnetic field, and residual magnetization in the electromagnet. The observed responses demonstrate significant hysteresis, as indicated by the variations in tip angular deflection with applied magnetic intensity, shown in figures 8-10. The hysteresis magnitude appears to escalate with increasing both the frequency and amplitude of the magnetic loading. Additionally, the data reveal saturation in response to magnetic flux densities over 15 mT. The results also point to complex nonlinear hysteresis behaviors for high amplitude magnetic excitations, such as cases C.9 and C.10. In contrast, at lower magnetic field strengths and frequencies, such as 5 mT and 1 Hz for case C.1, the hysteresis loop is nearly elliptical, reflecting the MSCR's linear viscoelastic behavior under low magnetic field amplitudes, as seen in Figure 8.

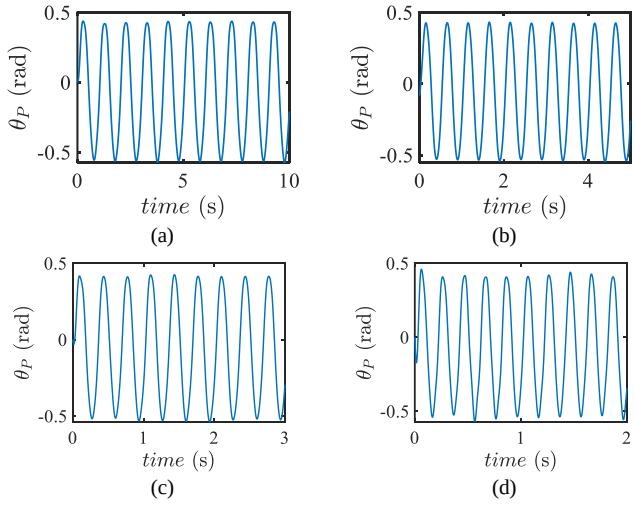

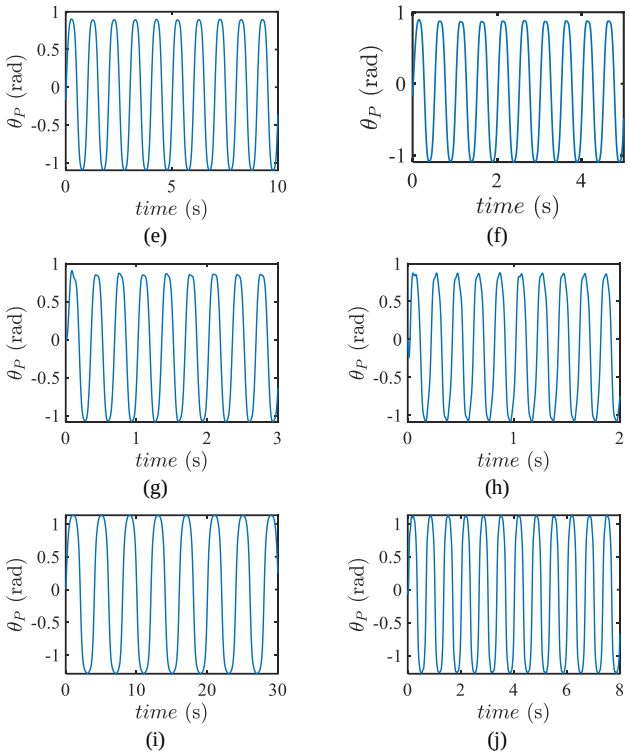

Figure 7. Time histories of tip deflection for cases: (a) C.1, (b) C.2, (c) C.3, (d) C.4, (e) C.5, (f) C.6, (g) C.7, (h) C.8, (i) C.9, (j) C.10.

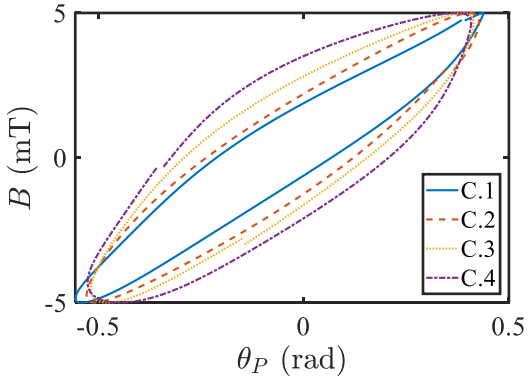

Figure 8. Hysteretic tip deflection responses obtained from the measurements for cases C.1 - C.4.

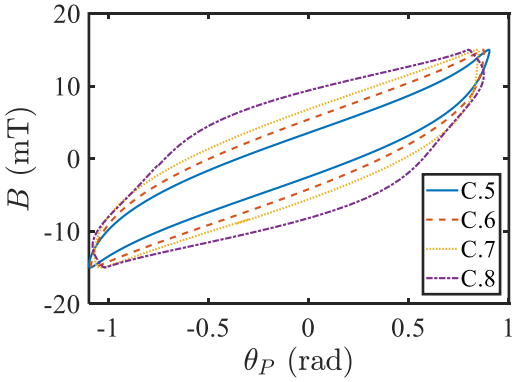

Figure 9. Hysteretic tip deflection responses obtained from the measurements for cases C.5 - C.8.

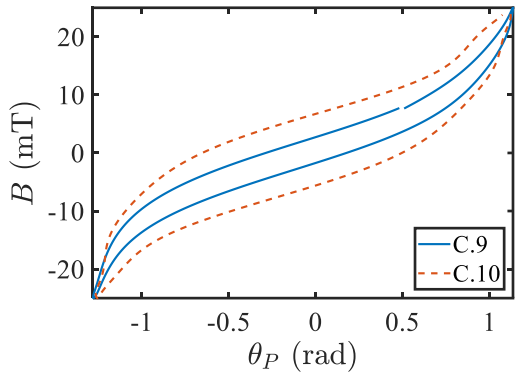

Figure 10. Hysteretic tip deflection responses obtained from the measurements for cases C.9 and C.10.

V. Conclusions

In this research, a HiL experiment was designed to investigate the large deflection response behavior of a cantilevered magnetic soft continuum robot submerged in a fluid environment under DC and AC magnetic intensities. The MSCR's residual magnetic flux density was assumed to align with the magnetic soft actuator's length in its rest configuration. The MSCR was fabricated using a silicone-based elastomer embedded with NdFeB particles, with a volume fraction of 20%, randomly dispersed within the elastomer. Laboratory tests, including tensile test, was conducted to ascertain the mechanical properties of the sample. The gathered experimental data from tensile test were then fitted with the Mooney-Rivlin hyperelastic model to calculate the MSCR's modulus of elasticity. The experiments revealed the MSCR's markedly nonlinear behavior, with a saturation trend at higher magnetic flux densities. Experimental results also demonstrated an increased hysteresis correlating with the rising frequency of the magnetic field.

Acknowledgment

Support from Natural Sciences and Engineering Research Council of Canada (NSERC) and FRQNT Doctoral Scholarship (B2X) are gratefully acknowledged.

References

[1] Y. Kim, X. Zhao, "Magnetic Soft Materials and robots," Chemical Reviews, vol. 122(5), pp. 5317–5364, , 2022.

[2] L. Wang, C. F. Guo, X. Zhao, "Magnetic Soft Continuum Robots with contact forces," Extreme Mechanics Letters, vol. 51, 101604, 2022.

[3] L. Wang, D. Zheng, P. Harker, A. B. Patel, C. F. Guo, X. Zhao, "Evolutionary design of Magnetic Soft Continuum Robots," Proceedings of the National Academy of Sciences, vol. 118(21), 2021.

[4] Y. Kim, G. A. Parada, S. Liu, X. Zhao, "Ferromagnetic soft continuum robots," Science Robotics, vol. 4(33), 2019.

[5] H. Zhu, Y. He, Y. Wang, Y. Zhao, C. Jiang, "Mechanically‐guided 4D printing of magnetoresponsive soft materials across different length scales," Advanced Intelligent Systems, vol. 4(3), 2100137, 2021.

[6] S. A. Moezi, R. Sedaghati, S. Rakheja, "An experimental investigation of dynamic motions of a small-scale magnetoactive soft robot undergoing large nonlinear movements," in Proceedings of SPIE, vol. 12483, 2023, pp. 124830N-1.

[7] R. Zhao, Y. Kim, S. A. Chester, P. Sharma, X. Zhao, "Mechanics of hard-magnetic soft materials," Journal of the Mechanics and Physics of Solids, vol. 124, pp. 244–263, 2019.

[8] S. A. Moezi, R. Sedaghati, S. Rakheja, "Nonlinear dynamic analysis and control of a small-scale magnetoactive soft robot," AIAA SCITECH 2022 Forum, 2022.

[9] W. Chen, Z. Yan, L. Wang, "On mechanics of functionally graded hard-magnetic soft beams," International Journal of Engineering Science, vol. 157, 103391, 2020.

[10] F. Dadgar-Rad, M. Hossain, "Large viscoelastic deformation of hard-magnetic soft beams," Extreme Mechanics Letters, vol. 54, 101773, 2022.

[11] C. Kadapa, M. Hossain, "A unified numerical approach for soft to hard magneto-viscoelastically coupled polymers," Mechanics of Materials, vol. 166, 104207, 2022.

[12] Z. Xing, H. Yong, "Dynamic analysis and active control of hard-magnetic soft materials," International Journal of Smart and Nano Materials, vol. 12(4), pp. 429–449, 2021.

[13] N. Nagal, S. Srivastava, C. Pandey, A. Gupta, A. K. Sharma, "Alleviation of residual vibrations in hard-magnetic soft actuators using a command-shaping scheme," Polymers, vol. 14(15), 3037, 2022.

[14] S. A. Moezi, R. Sedaghati, S. Rakheja, "Dynamic Modeling and Analysis of a Hard-Magneto-Viscoelastic Soft Beam under Large Amplitude Oscillatory Motions: Simulation and Experimental Studies," Nonlinear Dynamics, Apr 4:1-9, 2024.

[15] S. A. Moezi, R. Sedaghati, S. Rakheja, "Nonlinear dynamic modeling and model-based AI-driven control of a magnetoactive soft continuum robot in a fluidic environment," ISA Transactions, vol. 144, pp. 245-259, Jan. 2024.

[16] J. Bergström, "5 - Elasticity/Hyperelasticity," in Mechanics of Solid Polymers, J. Bergström, Ed. William Andrew Publishing, 2015, pp. 209-307. ISBN 9780323311502. Available: https://doi.org/10.1016/B978-0-323-31150-2.00005-4.